

Fast Tetrahedral Meshing in the Wild

YIXIN HU, New York University

TESEO SCHNEIDER, New York University

BOLUN WANG, Beihang University

DENIS ZORIN, New York University

DANIELE PANZZO, New York University

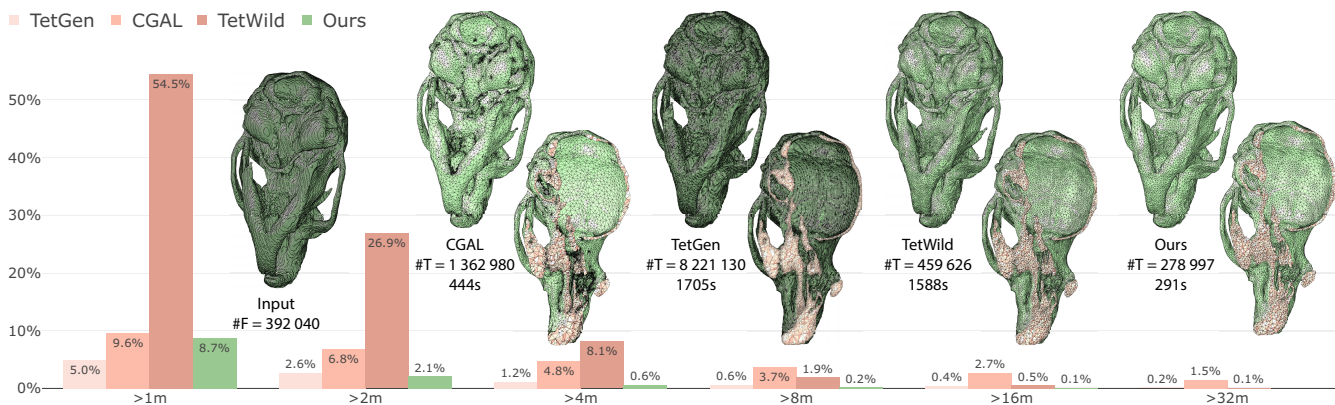


Fig. 1. A mouse skull model (from micro-CT) tetrahedralized by fTETWILD (right) compared with other popular tetrahedral meshing algorithms. The plot shows the percentage of models requiring more than a certain time for the different approaches over 4540 inputs (the subset of Thingi10k where all 4 algorithms succeed). Our algorithm successfully meshes 99.4% of the input models in less than 2 minutes, and processes all models within 32 minutes. The comparison has been done using the experimental setup of TetWild [Hu et al. 2018] and selecting a similar target resolution for all methods. The CGAL surface approximation parameter has been selected to be comparable to the envelope size used for TetWild and for our method.

We propose a new tetrahedral meshing technique, fTETWILD, to convert triangle soups into high-quality tetrahedral meshes. Our method builds upon the TetWild algorithm, inheriting its unconditional robustness, but dramatically reducing its computation cost and guaranteeing the generation of a valid tetrahedral mesh with floating point coordinates. This is achieved by introducing a new problem formulation, which is well suited for a pure floating point implementation and naturally leads to a parallel implementation. Our algorithm produces results qualitatively and quantitatively similar to TetWild, but at a fraction of the computational cost, with a running time comparable to Delaunay-based tetrahedralization algorithms.

ACM Reference format:

Yixin Hu, Teseo Schneider, Bolun Wang, Denis Zorin, and Daniele Panozzo. 2021. Fast Tetrahedral Meshing in the Wild. 1, 1, Article 1 (April 2021), 10 pages.

DOI: 10.1145/nnnnnnnn.nnnnnnnn

1 INTRODUCTION

Tetrahedral meshes are commonly used in graphics and engineering applications. The recently proposed Tetrahedral Meshing in the Wild [Hu et al. 2018] algorithm makes it possible to reliably tetrahedralize triangle soups by combining the exact, rational computations with a geometric tolerance to automatically address self-intersections or gaps in the input. The algorithm is extremely robust, opening the

door to automatic processing and repair of large collections of 3D models.

The algorithm has two downsides, one theoretical and one practical. The theoretical downside is that it does not guarantee the generation of a floating point tetrahedral mesh: the algorithm internally uses rational numbers, which are then converted to floating point in the process of mesh optimization. While quite unlikely, it is possible that the mesh optimization stage will be unable to round all coordinates of the output mesh to floating point. The practical downside is the long running time compared with Delaunay-based tetrahedralization algorithms. While this limitation is not a show-stopper for batch-processing, it severely limits the usability of TetWild in interactive or semi-interactive applications.

We introduce fTETWILD, a variant of the TetWild algorithm addressing both these limitations. Instead of generating a valid mesh using rational numbers and then rounding it to floating point during mesh optimization, we propose to start from an initial, coarse background tetrahedral mesh represented in floating point. We incrementally add one input triangle at a time, remeshing it locally and rejecting operations leading to meshes not representable in floating point. We then improve the quality of the mesh iteratively, and attempt to insert the rejected triangles into a higher quality mesh, for which the probability of failure is lower. The algorithm is thus always guaranteed to generate a valid floating point tetrahedral mesh: however it may not contain some of input triangles, which happens

rarely (2 models over 10 thousand) and only for close-to-degenerate input triangles with area less than 5e-8. The new algorithm can be implemented entirely using floating point coordinates, avoiding the higher runtime associated with rational numbers. The use of floating point numbers also simplifies parallelization, which we use during mesh optimization to further improve the runtime on large models.

The new algorithm is thus providing a stronger guarantee in terms of producing a valid floating point output mesh, compared to TetWild, while at the same time being much faster, with a runtime comparable to Delaunay-based algorithms (Figure 1). These improvements make it more practical, compared to TetWild, not only for volumetric meshing problems, but also for mesh repair and approximate mesh arrangements: by combining fTETWILD and some aspects of [Zhou et al. 2016], we obtain a mesh arrangement algorithm for imperfect input surfaces guaranteed to produce a valid floating point output. In contrast, the original algorithm presented in [Zhou et al. 2016] can fail due to invalid rounding after the arrangement computation. We demonstrate the robustness and practical utility of our algorithm on the Thingi10k dataset, plus a set of tests for approximate Booleans and for mesh repair. The complete reference implementation of fTETWILD is provided in the additional material, together with scripts to reproduce all results in the paper.

2 RELATED WORK

We briefly review the literature on tetrahedral meshing (Section 2.1), with an emphasis on envelope-based techniques, which are the one we build our algorithm on (we refer to [Cheng et al. 2012; Shewchuk 2012] for a more detailed overview of the topic). Then, we review mesh repair and mesh arrangement algorithms (Section 2.2), since our technique can be also used in these settings to enable processing of imperfect geometry.

2.1 Tetrahedral Meshing

Delaunay Meshing. The most studied and most widely used algorithms to generate tetrahedral meshes are based on the Delaunay condition [Alliez et al. 2005a; Aurenhammer 1991; Aurenhammer et al. 2013; Bishop 2016; Boissonnat et al. 2002; Boissonnat and Oudot 2005; Busaryev et al. 2009; Chen and Xu 2004; Cheng et al. 2008, 2012; Chew 1989, 1993; Cohen-Steiner et al. 2002; Dey and Levine 2008; Du and Wang 2003; Jamin et al. 2015; Murphy et al. 2001; Remacle 2017; Ruppert 1995; Sheehy 2012; Shewchuk 1996, 1998, 1999, 2002; Si 2015; Si and Gartner 2005; Si and Shewchuk 2014; Tournois et al. 2009]. These methods are efficient and are widely used in commercial software. They can be applied to either point clouds inputs, or to tessellate the interior of clean, manifold, non self-intersecting discrete surfaces. Unlike our method, they are, unfortunately, not designed to deal with imperfect input, making them fail often on data *in the wild* [Hu et al. 2018].

Grid Methods. An alternative approach is the use of a background grid [Baker et al. 1988; Bern et al. 1994; Bridson and Doran 2014; Bronson et al. 2013; Doran et al. 2013; Labelle and Shewchuk 2007; Molino et al. 2003; Yerry and Shephard 1983]: these algorithms start by filling the entire bounding box of the input with a regular lattice

or with a hierarchical space partitioning, optionally intersect the background mesh with the input surface, and then discard the elements outside of the input. These methods are simpler and more robust than Delaunay methods, but still struggle with imperfect input geometry, and create high-quality elements only in the interior of the mesh, where the background mesh is preserved exactly. Unfortunately, placing badly shaped triangles on the boundary is problematic for many applications. Our algorithm borrows the idea of a background mesh, but insert the elements incrementally, interleaving mesh optimization stages to ensure that the final quality of the mesh is uniformly high. We also use the generalized winding number [Barill et al. 2018; Jacobson et al. 2013] as a filtering criteria to handle imperfect input.

Front-Advancing Methods. Another family of methods starts from the boundary, and inserts one element at a time, growing the volumetric mesh (i.e. marching in space), until the entire volume is filled [Alauzet and Marcum 2014; Cuilliere et al. 2013; George 1971; Haimes 2014; Peraire et al. 1987; Sadek 1980]. These methods create high quality elements close to the boundary, but introduce bad elements in the interior regions where the fronts meet.

Envelope Meshing. All methods discussed above assume a valid, manifold, non self-intersecting boundary input mesh, and are not designed to handle the imperfections which are common in real-world CAD and scanned data. This issue has been tackled for surface meshes in Mandad et al. [2015] by creating a surface approximation within a tolerance volume using a modified Delaunay refinement process. A similar idea has been exploited for volumetric meshing in TetWild [Hu et al. 2018], and its 2D counterpart TriWild [Hu et al. 2019]. Their core idea is a combination of exact computation, using a hybrid kernel similar to [Attene 2017], and a surface envelope [Hu et al. 2017], which allows the resulting mesh to approximate the input instead of reproducing it exactly. Our method closely follows [Hu et al. 2018], but we design our algorithm to avoid the use of exact computation, and to allow parallelization of the most expensive steps. We compare the two techniques in Section 4.2.

Mesh Improvement. Many algorithms have been proposed to improve the quality of an existing tetrahedral mesh by displacing vertices or changing the local connectivity [A. Freitag and Ollivier-Gooch 1998; Alexa 2019; Alliez et al. 2005b; Canann et al. 1996, 1993; Chen and Xu 2004; Faraj et al. 2016; Feng et al. 2018; Hu et al. 2018; Lipman 2012]. Our method relies on the algorithm proposed in Hu et al. [2018], which uses a set of local operations to optimize the conformal AMIPS energy [Fu et al. 2015; Rabinovich et al. 2017]. We parallelized some of the steps of their algorithm (Section 3), which is easier in our case since we only have floating point coordinates.

2.2 Applications

Mesh Repair. Repairing damaged triangle meshes is an important topic in geometry processing. Since our algorithm can be used for this purpose, we review the most recent works in this direction, and we refer to [Attene et al. 2013] for a complete overview.

MeshFix [Attene 2010, 2014] detects problematic regions in triangle meshes, and uses a set of local operations to heal them. The tool is very effective, but due to its greedy nature it might delete

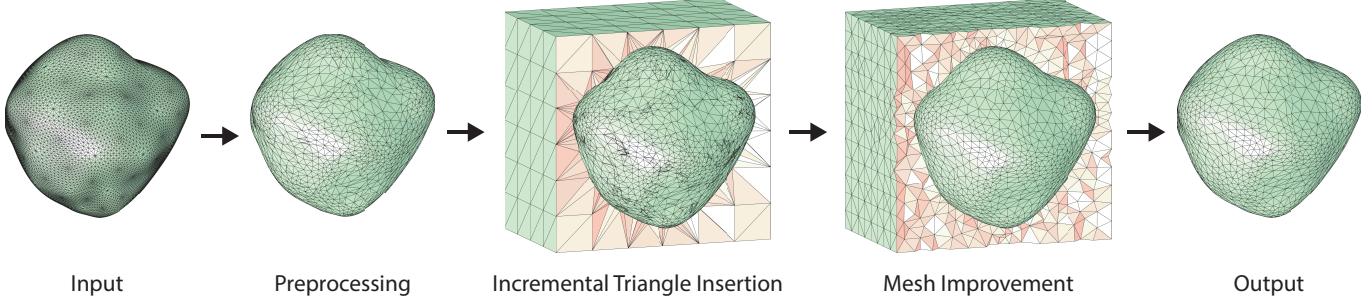


Fig. 2. Overview of our algorithm. From left to right, the input mesh is simplified, a background mesh is created and the input faces are inserted, the mesh quality is optimized, and the final result is obtained by filtering the elements lying outside the input surface.

large parts on a mesh. The most recent mesh repair technique has been introduced in [Hu et al. 2018]: the algorithm generates a tetrahedral mesh and discards the generated tetrahedra, only keeping the boundary surface. While simple and effective, this technique is computationally expensive, and thus only usable in batch processing applications. Our algorithm can be used in the same way, but its higher efficiency makes it more practical.

Booleans and Mesh Arrangements. Many approaches to performing Boolean operations on meshes were proposed, some emphasizing robustness, other exact results, and other performance. In most cases, non-trivial assumptions are made on the input meshes: most commonly, these are required to be closed; in other cases, no self-intersections are allowed, or most restrictively vertices may be assumed in general position.

CGAL, one of the most robust implementations of Boolean operations available [Granados et al. 2003], relies on exact arithmetic, and uses a very general structure of Nef polyhedra [Bieri and Nef 1988] to represent shapes. This allows one to obtain exact Boolean results in degenerate cases (e.g., when the result is a line or a point). At the same time, the assumptions on the input are quite restrictive: the surfaces need to be closed and manifold (although the latter constraint could be eliminated).

Another approach to achieve robustness at the expense of accuracy, is to convert input meshes to level sets e.g. by sampling a signed distance function for each object [Museeth et al. 2002] and perform all operations on the level set functions. The obvious disadvantage of these methods is that their accuracy is limited by the resolution of the grid; the original mesh geometry is lost, and it is non-trivial to maintain even explicitly tagged features. These downsides are partially addressed by adaptive [Varadhan et al. 2004] and hybrid [Pavlic et al. 2010; Wang 2011; Zhao et al. 2011], the latter preserving mesh geometry away from intersections. All these methods rely on well-defined signed distance function, i.e., assume that input meshes are closed, and may still significantly alter the input geometry near intersections. [Schmidt and Singh 2010] does not use a signed distance function, but resembles these methods, in that it removes existing geometry near intersections and replaces it by new mesh connecting the two objects and approximating the result of the Boolean. BSP-based methods, starting from [Naylor et al. 1990; Thibault and Naylor 1987] are closest in their approach to ours. Using BSP preserves the input much more accurately, and, along

the way, creates a volume partition. However, it is prone to errors due to numerical instability of intersection calculations, and due to global intersections performs excessive refinement. [Bernstein and Fussell 2009] addresses the issue of non-robustness by using exact predicates, and [Campen and Kobbett 2010] reduces refinement by creating localized BSP trees in an octree. Examples of highly efficient but non-robust software for computing Booleans are [Douze et al. 2015], [Barki et al. 2015], and [Bernstein 2013]. A general position assumption is often required explicitly or implicitly. In [Zhou et al. 2016] a robust way to compute *mesh arrangements* is introduced, which, in particular, allows one to perform Boolean operations robustly. Robustness is achieved by using rational numbers for critical computations. To perform Booleans the mesh is required to be PWN, which does not always hold in meshes in the wild [Zhou and Jacobson 2016].

Sheng et al. [2018a,b] use a combination of plane-based and vertex-based representations of mesh faces to improve robustness of basic operations needed for Boolean operations performed in floats. The method achieves very high efficiency, at the expense of somewhat lower robustness compared to the state of the art. The method assumes that the input meshes enclose solids and are free of self-intersections. [Magalhães et al. 2017] is an efficient technique using simulation-of-simplicity techniques to handle general intersections between objects, self-intersections or holes are not handled. [Paoluzzi et al. 2017] considers a general problem of arrangements of complexes in 2D and 3D, presenting a theoretical general merge algorithm, but do not consider the questions of robustness and handling imperfect inputs.

Compared to existing methods, the application of fTETWILD to Boolean operations is more conservative, in terms of mesh geometry changes and refinement, compared to level set and BSP-based methods, while maintaining their level of robustness. At the same time, thanks to the geometric tolerance, fTETWILD is capable of eliminating near-degenerate or overly refined triangles in the input model, which [Zhou et al. 2016] cannot do. We also make fewer assumptions on the inputs, allowing gaps, self-intersections, and degeneracies.

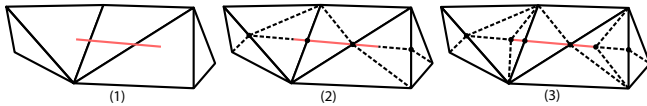


Fig. 3. Two-dimensional illustration of our triangle insertion algorithm. A red edge cuts through the intersecting triangles (1), the topology is constructed to ensure a valid mesh using the table mapping boundary edge intersection to internal connectivity (2), and finally the endpoints are preserved with an edge arrangement (3).

3 METHOD

fTETWILD converts an input triangle soup represented in floating points numbers into an inversion-free tetrahedral mesh also represented in floating points, while trying to keep the faces of the tetrahedral mesh within an user-defined envelope ϵ from the input triangles. This is achieved by starting from a background tetrahedral mesh, and iteratively inserting the input triangles into the current mesh by splitting its elements. Each split generates a new inversion-free tetrahedral mesh that preserves the newly inserted triangle as a collection of faces. Note that this procedure could (and will) fail due to floating point rounding; in these cases we remove the face causing the failure (i.e. introducing an inverted element due to rounding), and postpone the insertion of the triangle to a later stage of the algorithm, when the quality of the mesh has increased.

This procedure resembles the algorithm proposed in [Hu et al. 2018], but with two key differences: (1) it maintains the same level of robustness, measured on the Thingi10k benchmark, as TetWild without requiring the use of rational numbers and (2) it does not use intermediate polyhedral elements. These differences guarantee the generation of an inversion-free tetrahedral mesh in floating points at every stage of the algorithm, with a potential drawback of not being able to insert all input faces.

Overview. The algorithm takes as input a triangle soup with two user-defined parameters: target edge length ℓ , and envelope size ϵ for geometric tolerance. The ϵ -envelope represents the maximal deviation from the input surface the user is willing to accept. For instance, in additive manufacturing applications ϵ can be the machining precision.

Our algorithm consists of 4 phases (Figure 2): (1) the input triangles soup is initially simplified while ensuring it fits in the ϵ -envelope (Section 3.1), (2) a background mesh is then generated, and the simplified triangles are iteratively inserted into it if they do not lead to numerical problems (Section 3.2), (3) the mesh is improved using local operations (Section 3.3), and at the end of each improvement stage we reattempt the insertion of missing input triangles, (4) the mesh is optionally filtered (Section 3.4), to remove the outer mesh or to perform Boolean operations.

During the whole procedure we ensure that the floating point tetrahedral mesh remains *valid*. That is, (1) each element has positive volume (checked using exact predicates [Lévy 2019; Shewchuk 1997]) and (2) each successfully inserted triangle is preserved inside the ϵ -envelope.

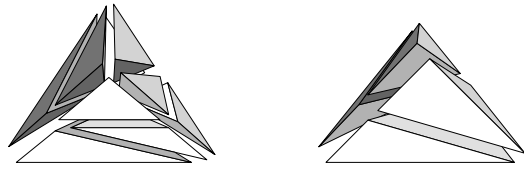


Fig. 4. Additional edge cutting configurations required by our algorithm.

3.1 Preprocessing

We use the same procedure proposed in [Hu et al. 2018]: we merge vertices closer than a numerical tolerance $1e-8$, and collapse edges if (1) their incident edges are manifold, and (2) the collapse does not move triangles outside of the ϵ -envelope. Note that in the simplification we use a more conservative envelope (i.e., we keep the simplified surface closer than ϵ to the input) to facilitate snapping in triangle insertion, as explained in Section 3.2.

Since this step is computationally expensive for massive models, we propose a simple parallelization strategy which leads, on average, to a 4x speedup. We do a serial 2-coloring pass over all input faces: all triangles are initially white, then we iterate over all edges and color their incident triangles black if all the triangles are white. Then we attempt to collapse in parallel all edges with only black incident triangles. Finally, we iterate this procedure until we are unable to collapse more than 0.01% of the input vertex count.

3.2 Incremental Triangle Insertion

Background Mesh Generation. An initial, non-conforming tetrahedral mesh is generated using Delaunay tetrahedralization [Lévy 2019] on the vertices of the simplified input triangle soup enriched with additional voxel points [Hu et al. 2018]. Other options (e.g., a regular lattice) can also be used, but we found Delaunay tetrahedralization preferable since a significant subset of the input faces naturally appears in the background mesh, thus not requiring insertion.

Single Triangle Insertion. The key component of our algorithm is the insertion of one triangle into a valid tetrahedral mesh, changing its connectivity, and adding vertices and tetrahedra as required. We propose a three-stage algorithm (Figure 3) borrowing ideas from marching tetrahedra [Doi and Koide 1991] and marching cubes [Lorensen and Cline 1987]: we generate a table of volumetric tessellations, hashed by detecting the 6 intersections with the edges of each tetrahedra, and which is used to efficiently construct the topology of the new mesh. Unfortunately, there are ambiguous configurations (e.g., when the cut generates a quadrilateral), which needs to be handled by ensuring consistency across neighbors.

Table Generation. A plane cutting a single tetrahedron can intersect it in a finite number of ways, which can be encoded uniquely by tracking the intersection between the plane and the edges. There is a total of 2^6 configurations, many of which are redundant due to symmetry: some are technically impossible but we still consider them since they can arise when consistency is enforced. To cover all edge intersection configurations required by our algorithm, there are 6 unique tetrahedral decompositions: 4 were introduced in [Schweiger

and Arridge 2016], and 2 additional ones required to cover the remaining cases (Figure 4), leading to a total of 41 possible combinations including symmetries. We enumerate these 41 configurations and generate a table mapping boundary edge intersections to the connectivity required to fill the tetrahedron with sub-tetrahedra matching the boundary splits. We provide the table containing the 41 configurations in the additional material and the code to generate them.

Hash Generation. To insert a triangle T in the current tetrahedral mesh, the algorithm first detects all the tetrahedra containing at least a point of T , and then cuts their edges using the plane containing T . This cut generates 6 flags for each touched tetrahedra (including those in the one-ring of the intersected tetrahedra) indicating which edge is intersected with the plane. We then use the 6 flags with the aforementioned connectivity table to tessellate the tetrahedra. Note that cutting a triangular face with a plane might create a quadrilateral, which can be triangulated in 2 distinct ways and it is important to consistently pick one of the two on both sides of the quadrilateral (we select the one leading to a maximal minimal volume of the involved tetrahedra), to ensure a valid connectivity.

Snapping. This insertion algorithm is straightforward to implement using exact constructions with rational coordinates, but becomes challenging in our setting due to floating point rounding, and may fail, resulting in a triangle being rejected. To reduce the probability of rejections, we perform two types of snapping: (1) we snap intersections which are close to vertices (i.e., with a distance less than $1e-3\epsilon$), since these intersections would lead to sliver elements, and (2) we snap the entire intersection plane to one of the edges/faces of the tetrahedra if the plane to edge/face distance is smaller than $1e-3\epsilon$. These two operations reduce the chances of introducing degenerate or flipped elements, but cannot guarantee their absence. If we detect a degenerate or inverted element (using exact predicates) in the new topology, we rollback this insertion and postpone it to later stages of the algorithm, after the quality of the mesh has been improved by local optimization.

2D Arrangements. Cutting the tetrahedral mesh is not sufficient to ensure that the input triangle T is a face of the tetrahedral mesh. For instance, if the triangle is entirely contained inside a tetrahedron (see inset), the result of the cutting will be a “larger triangle”. This is avoided by performing additional cuts, which ensure that the edges of T are in the tetrahedral mesh. For every edge of T , we first check if it is already present (i.e., another triangle cuts through it) or its incident triangle is coplanar. In both cases there is no need to perform additional cuts, since the edge is either present or unnecessary. In the remaining case (i.e., the edge should be present but it is not) we compute the intersection between the line passing through it and the edges of the tetrahedron face. This procedure generates yet again an “edge tagging” which we use with the table above to create a valid decomposition of the tetrahedron. To make the computation of intersection stable, we project the line and the triangles on the best-fitting axis-aligned

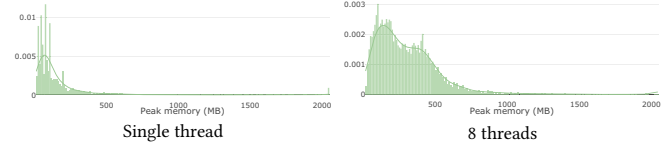
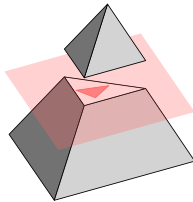


Fig. 5. Histogram of memory usage of FTetWild over the Thingi10k dataset.

plane leading to a 2D intersection test. Note that these cuts might fail due to numerical reasons, in this case we rollback the operation and postpone the insertion to later stages.

3.3 Mesh Improvement

We adapt the mesh improvement framework proposed in TetWild [Hu et al. 2018], optimizing the AMIPS 3D energy [Rabinovich et al. 2017] to increase the mesh quality, but avoid the overhead introduced by the hybrid kernel by specializing the framework for floating point computation. There are only two algorithmic differences: (1) we parallelize the vertex smoothing step using a graph coloring strategy, and (2) we add an extra step attempting to insert any input faces that were not inserted before.

The mesh improvement terminates when either a user-specified mesh quality or a user-controlled number of iterations is reached. To ensure a fair comparison, for the large dataset testing and all examples in the paper, we use the same stopping criteria (max AMIPS energy is smaller than 10 or the number of optimization iterations reaches 80), and input parameters $\epsilon = 1e-3d$ and $\ell = d/20$ (d is the diagonal’s length of bounding box of the input mesh) as TetWild [Hu et al. 2018].

3.4 Filtering

The output of the mesh improvement step is a volumetric tetrahedral mesh of the bounding box of the input triangle soup, with preprocessed input triangles inserted. We provide two ways of optionally process the result for final output, targeting two different applications. The first strategy uses the generalized winding number [Jacobson et al. 2013] to filter the tetrahedra outside of the preserved/tracked input [Hu et al. 2018]. The second application is a volumetric extension of the mesh arrangement algorithm [Zhou et al. 2016]. In this case, the input becomes a set of triangle soups, coupled with a set of Boolean operations to perform on them. During triangle insertion stage, we keep track of the provenance of each triangle, and use it at the end to compute a set of generalized winding numbers (one for each tracked input surface) for the centroids of all tetrahedra in the volumetric mesh. We use the set of winding numbers to decide which tetrahedron to keep by checking if it is supposed to be contained in the result of the Boolean operation. For instance, when intersecting two triangle soups, we keep all tetrahedra that are inside (according to the winding number) both input triangle soups. The advantage of this method is that Boolean operations can process non-PWN surfaces, and the output comes optionally equipped with a tetrahedral mesh, which could be useful in downstream applications.

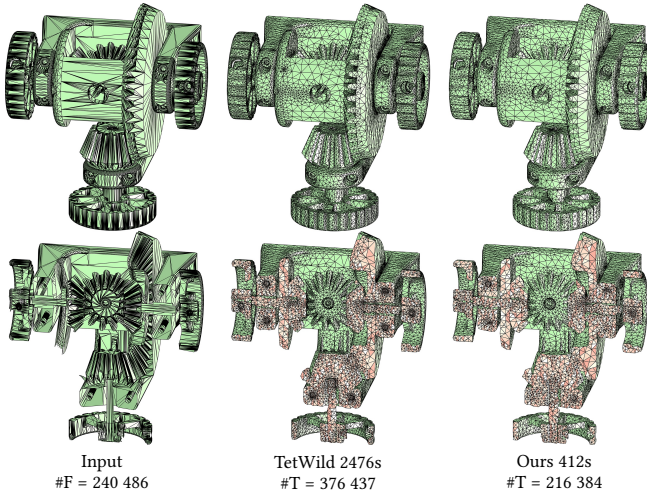


Fig. 6. Our method (right) produces high-quality tet-meshes that are similar to TetWild (middle). The maximal AMIPS energy over all tetrahedra are also close (8.0 and 8.1 respectively).

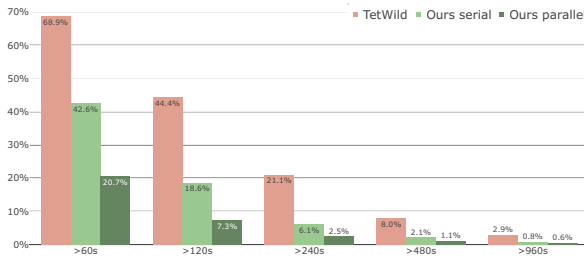


Fig. 7. Percentage of models requiring more than a certain time for our parallel and serial algorithm compared with TetWild on Thingi10k dataset.

4 RESULTS

Our algorithm is implemented in C++ and it has been optimized to improve the timing performance. We use Eigen [Guennebaud et al. 2010] for linear algebra routines. We perform a large-scale test of our method on the Thingi10k dataset [Zhou and Jacobson 2016], which contains ten thousand real-world surface triangle meshes, using cluster nodes with a Xeon E5-2690v4 2.6GHz, limiting every job to 8 threads, running time to 12 hours, and maximum memory to 128GB. Within these constraints fTETWILD successfully tetrahedralize 9998 models (single-threaded) and 9999 models (8 threads) out of 10000 input. Most of the input models can be tetrahedralized with less than 1GB of RAM (multi-threaded) or 500MB (single-threaded) as detailed in Figure 5. Very complex models might require more memory, for instance the one in Figure 11 uses around 22GB of memory. The reference implementation and the scripts used to generate the results are attached to the submission and will be released as an open-source project.

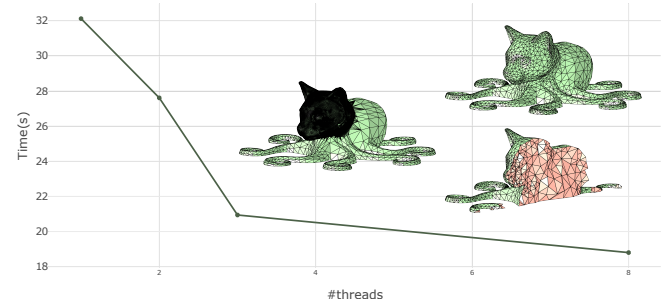


Fig. 8. Scaling experiment on an input mesh with 37884 faces (middle). The outputs with different threads have similar mesh size and mesh quality. The output (right) created with 8 threads has 15124 tetrahedra and 8.3 max AMIPS energy.

4.1 Large Scale Comparison

We compare the running time on the 4540 models where TetWild [Hu et al. 2018], TetGen [Si 2015], and CGAL [Wein et al. 2018] all succeed. In average, our method is 35% slower (29s) than the state-of-the-art, Delaunary-based tetrahedral mesher TetGen (22s), and it is faster than both CGAL (94s) and TetWild (106s). Figure 1 shows the number of models requiring more than a given time: in less than 4 minutes our method successfully tetrahedralize 99.4% of the inputs. It is interesting to note that the tail of the distribution of our method is shorter than both TetGen and CGAL. For instance, there are only 3 models where our method requires more than 16 minutes, differently from TetGen, CGAL, and TetWild which have 20, 121, and 24 models, respectively.

4.2 Differences and Similarities with TetWild

Our method is inspired by the TetWild algorithm [Hu et al. 2018], sharing many similarities, but also important differences.

Problem Statement. While both algorithms generate tetrahedral meshes starting from a triangle soup and produce a qualitatively and quantitatively similar output (Figure 6), the problem they solve (and possible failures) are different. TetWild is guaranteed to generate a tetrahedral mesh that has a set of faces contained within the envelope of the input, but the resulting mesh might not be roundable to floating points, leading to an unusable mesh in downstream applications. In contrast, our algorithm is guaranteed to produce a valid tetrahedral mesh with floating point coordinates, but might fail to insert some faces of the input, leading to a violation of the envelope condition.

Parallelization and Running Times. While technically possible, parallelizing TetWild is challenging due to the hybrid kernel used: each operation might be performed either in rational or floating point depending on the coordinate of the vertices involved, making vectorization and parallelization more difficult. Since our algorithm uses only floating point numbers, it is easier to parallelize. We compare the running times over the Thingi10k dataset with and without parallelization in Figure 7. Our algorithm is, on average, 4 times faster than TetWild (62s in average versus 241s) on a machine with 8 cores. Figure 8 shows the parallel scaling of our algorithm on

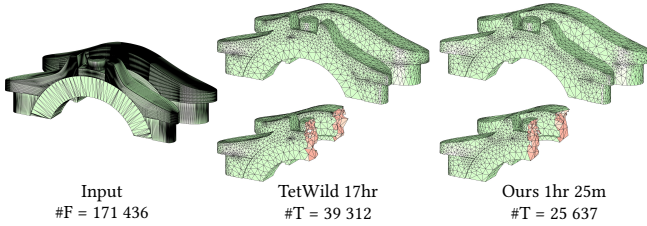


Fig. 9. Example of a challenging model where fTETWILD is 12 times faster than TetWild. The maximal AMIPS energy of TetWild and fTETWILD is 1625.4 and 18.1 respectively.

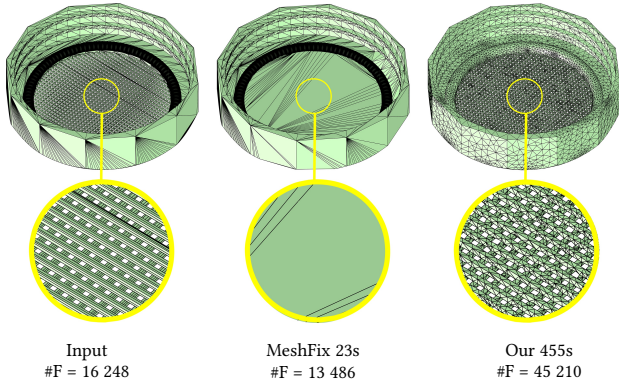


Fig. 10. Example of repairing an invalid triangular mesh (left) with MeshFix (middle) and our algorithm (right). MeshFix is fast but loses details during processing, while our method preserves them. The max AMIPS energy of our intermediate tetrahedral mesh is 7.8.

a medium-sized input. On the time-consuming example in Figure 9 our method is up 12 time faster of TetWild.

4.3 Mesh Repair

Similarly to TetWild, our algorithm can be used to repair imperfect triangle meshes by tetrahedralizing the volume and extracting the surface of generated tetrahedral mesh. Differently from TetWild, the mesh improvement step of our method (Section 3.3) can be stopped at any time since we always ensure to have an inversion-free floating point tetrahedral mesh during all the stages of our algorithm. High tetrahedral mesh quality is not required for this application, and we can thus stop mesh optimization as soon as all input faces are inserted, further reducing the running time. We compared our result with the state-of-the-art mesh repairing tool MeshFix [Attene 2010] in Figure 10, where our method, while slower, provides a superior and more reliable result.

We also tested an extremely challenging model coming from an industrial application in additive manufacturing (the part is copyrighted by Velo3D): the design of an exhaust pipe using a volume filled with a structure based on the gyroid triply periodic minimal surface. The model has a multitude of issues introduced during the modeling phase, but it can be cleaned up by our algorithm within 54 minutes (or 98 minutes with half default envelope), compared to the around 2 weeks of manual labor required by their current

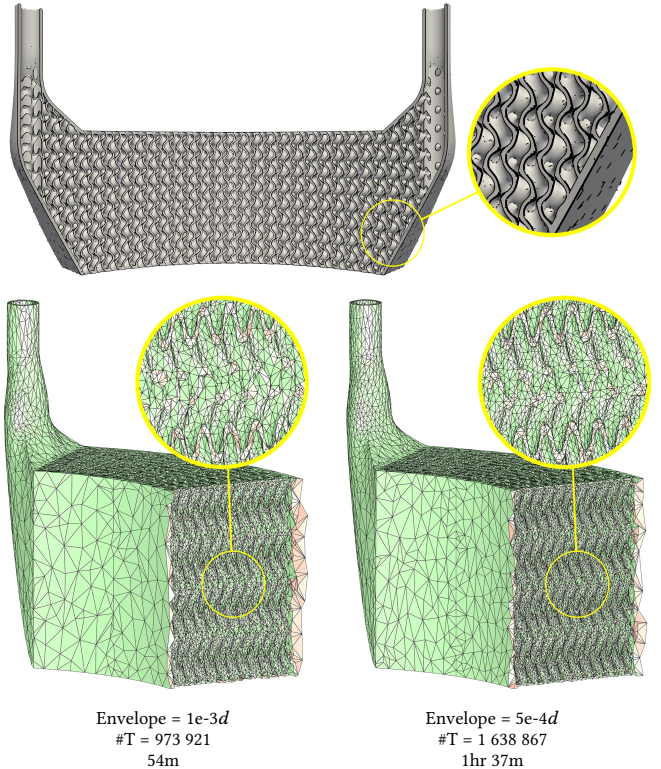


Fig. 11. Meshing a complex model with 93 million vertices and 31 million faces with different envelope sizes (top). The input mesh contains degenerate triangles and severe self-intersections. Our output tetrahedral meshes have max AMIPS energy at 130 (bottom, left) and 90 (bottom, right).

processing pipeline. Our output mesh is directly usable for FEA (Figure 11), further editing, or fabrication. As a reference point, the original implementation of TetWild takes 215 minutes with default envelope size.

The recently proposed a priori p -refinement [Schneider et al. 2018] is an ideal fit for our approach when targeting FEM applications. [Schneider et al. 2018] provides a simple formula to determine the degree of the base of each element to compensate for its, possibly bad, shape. We can use this criteria to terminate the mesh optimization early in our algorithm, as we show in the example in Figure 12.

4.4 Mesh Arrangements

Zhou et al. [2016] proposes to compute the arrangement between multiple surfaces using a clever algorithm to map Boolean operations into simple algebraic expressions involving the winding number of the input surfaces. Their method is robust, but only supports clean PWN surfaces as input. We propose a simple extension of their algorithm (Section 3.4) to arbitrary triangle soups, by exploiting our volumetric discretization: we replace the surface arrangement with the arrangement of tetrahedral meshes, and replace the winding number with the generalized winding number over the input tetrahedra soup (thresholded at 0.5).

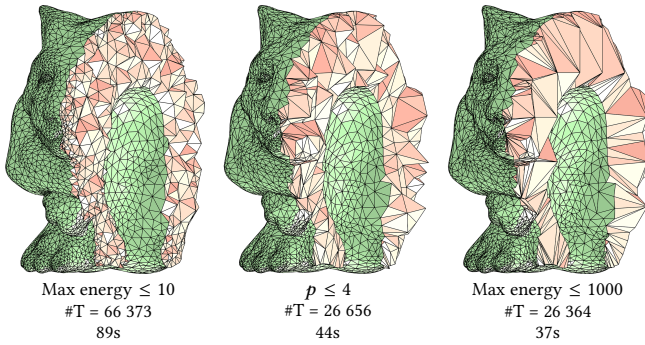


Fig. 12. Different stopping criteria of our algorithm. The full optimization reduces the AMIPS energy to 9.4 (left). For FEM applications, Schneider et al. [2018] proposes to stop the optimization when the maximum a priori p -refinement required is 4 (middle), resulting in a faster meshing and lower runtime and lower mesh quality (max AMIPS energy 80.3). For mesh repair, the quality of the tet-mesh (and surface mesh) is usually not relevant (right) and the optimization can be stopped as soon as all the input faces are inserted (max AMIPS energy 368.9).

The advantages of our method is evident when the input surfaces come from CAD models containing small gaps or self-intersections: Both Mesh Arrangements Zhou et al. [2016] and CGAL [Hachenberger and Kettner 2019] are unable to perform the operation (since it is not well defined for non-PWN surface), while fTETWILD can compute an approximate (since it allows for an ϵ -deviation from the input surfaces) union, difference, and intersection between them (Figure 13), providing robust (but slower) Boolean operations on imperfect geometry.

The intermediate tetrahedral mesh generated to compute the Boolean operation is useful for some downstream applications. For example, a high-quality volumetric mesh is required for simulating the fluid flow on a cylindrical tube containing an obstacle (Figure 14): our algorithm creates it while computing the Boolean difference between the two, and the mesh is directly usable for fluid simulation.

5 LIMITATIONS AND CONCLUDING REMARKS

We introduced fTETWILD, a novel robust tetrahedral meshing algorithm for triangle soups which combines the robustness of TetWild with a running time comparable to Delaunay-based methods. The improved performance makes this algorithm suitable not only for applications requiring a volumetric discretization, but also for surface mesh repair and Booleans. The algorithm uses only floating point computation, making it simpler to parallelize and enabling deployment on hardware platforms lacking robust rational implementations (such as javascript/webassembly).

Our current parallelization approach shows that our algorithm benefits from shared-memory parallelization; exploring more advanced parallelization techniques and extending it to distributed computation on HPC clusters are exciting directions for future work. Our iterative triangle insertion algorithm could be used in dynamic remeshing tasks, potentially allowing to reuse an existing mesh and insert new faces only in regions with high deformation. While conceptually trivial, extending our algorithm to 2D triangle meshing could improve the performance of [Hu et al. 2019].

Our algorithm uses the conformal AMIPS energy [Rabinovich et al. 2017] to measure and optimize the quality of the tetrahedra. An interesting alternative has been introduced concurrently to our work by [Alexa 2019]: they propose to optimize directly for the Dirichlet energy of the tetrahedralization and show that this measure is effective at removing slivers, while being computationally efficient to evaluate. A comparative study of the two measures would be interesting, and using the Dirichlet energy could lead to further reductions in the running time of our method.

REFERENCES

L. A. Freitag and C. Ollivier-Gooch. 1998. Tetrahedral Mesh Improvement Using Swapping and Smoothing. *Internat. J. Numer. Methods Engrg.* 40 (05 1998). DOI: [https://doi.org/10.1002/\(SICI\)1097-0207\(19971115\)40:213.0.CO;2-9](https://doi.org/10.1002/(SICI)1097-0207(19971115)40:213.0.CO;2-9)

F. Alauzet and D. Marcum. 2014. A Closed Advancing-Layer Method With Changing Topology Mesh Movement for Viscous Mesh Generation. In *Proceedings of the 22nd International Meshing Roundtable*. Springer International Publishing, Cham, 241–261. DOI: https://doi.org/10.1007/978-3-319-02335-9_14

M. Alexa. 2019. Harmonic Triangulations. *ACM Transactions on Graphics (Proceedings of SIGGRAPH)* 38, 4 (2019), 54.

P. Alliez, D. Cohen-Steiner, M. Yvinec, and M. Desbrun. 2005a. Variational Tetrahedral Meshing. *ACM Transactions on Graphics* 24, 3 (07 2005), 617. DOI: <https://doi.org/10.1145/1073204.1073238>

P. Alliez, D. Cohen-Steiner, M. Yvinec, and M. Desbrun. 2005b. Variational Tetrahedral Meshing. *ACM Trans. Graph.* 24, 3 (July 2005), 617–625. DOI: <https://doi.org/10.1145/1073204.1073238>

M. Attene. 2010. A lightweight approach to repairing digitized polygon meshes. *The Visual Computer* 26, 11 (01 Nov 2010), 1393–1406. DOI: <https://doi.org/10.1007/s00371-010-0416-3>

M. Attene. 2014. Direct Repair of Self-intersecting Meshes. *Graph. Models* 76, 6 (Nov. 2014), 658–668. DOI: <https://doi.org/10.1016/j.gmod.2014.09.002>

M. Attene. 2017. *ImatiSTL - Fast and Reliable Mesh Processing with a Hybrid Kernel*. Springer Berlin Heidelberg, Berlin, Heidelberg, 86–96.

M. Attene, M. Campen, and L. Kobbelt. 2013. Polygon Mesh Repairing: An Application Perspective. *ACM Comput. Surv.* 45, 2, Article 15 (March 2013), 33 pages. DOI: <https://doi.org/10.1145/2431211.2431214>

F. Aurenhammer. 1991. Voronoi Diagrams—a Survey of a Fundamental Geometric Data Structure. *ACM Comput. Surv.* 23, 3 (Sept. 1991), 345–405. DOI: <https://doi.org/10.1145/116873.116880>

F. Aurenhammer, R. Klein, and D.-T. Lee. 2013. *Voronoi Diagrams and Delaunay Triangulations*. WORLD SCIENTIFIC, River Edge, NJ, USA. DOI: <https://doi.org/10.1142/8685>

B. S. Baker, E. Grosse, and C. S. Rafferty. 1988. Nonobtuse triangulation of polygons. *Discrete & Computational Geometry* 3, 2 (01 Jun 1988), 147–168. DOI: <https://doi.org/10.1007/BF02187904>

G. Barill, N. Dickson, R. Schmidt, D. I. Levin, and A. Jacobson. 2018. Fast Winding Numbers for Soups and Clouds. *ACM Transactions on Graphics* 37, 4 (2018), 43:1–43:12.

H. Barki, G. Guennebaud, and S. Foufou. 2015. Exact, robust, and efficient regularized Booleans on general 3D meshes. *Computers and Mathematics with Applications* 70, 6 (2015), 1235–1254.

M. Bern, D. Eppstein, and J. Gilbert. 1994. Provably good mesh generation. *J. Comput. System Sci.* 48, 3 (1994), 384 – 409. DOI: [https://doi.org/10.1016/S0022-0005\(80\)9059-5](https://doi.org/10.1016/S0022-0005(80)9059-5)

G. Bernstein. 2013. Cork Boolean Library . (2013). <https://github.com/gilbo/cork>.

G. Bernstein and D. Fussell. 2009. Fast, Exact, Linear Booleans. In *SGP: Eurographics Association*, Aire-la-Ville, Switzerland, Switzerland, 1269–1278.

H. Bieri and W. Nef. 1988. Elementary Set Operations with D-dimensional Polyhedra. In *Proc. IWCGA*. Springer-Verlag, Berlin, Heidelberg, 97–112.

C. J. Bishop. 2016. Nonobtuse Triangulations of PSLGs. *Discrete & Computational Geometry* 56, 1 (2016), 43–92.

J.-D. Boissonnat, O. Devillers, S. Pion, M. Teillaud, and M. Yvinec. 2002. Triangulations in CGAL. *Computational Geometry* 22 (2002), 5–19.

J.-D. Boissonnat and S. Oudot. 2005. Provably Good Sampling and Meshing of Surfaces. *Graphical Models* 67, 5 (09 2005), 405–451. DOI: <https://doi.org/10.1016/j.gmod.2005.01.004>

R. Bridson and C. Doran. 2014. Quartet: A tetrahedral mesh generator that does isosurface stuffing with an acute tetrahedral tile. <https://github.com/crawfordoran/quartet>. (2014).

J. R. Bronson, J. A. Levine, and R. T. Whitaker. 2013. Lattice Cleaving: Conforming Tetrahedral Meshes of Multimaterial Domains With Bounded Quality. In *Proceedings of the 21st International Meshing Roundtable*. Springer Berlin Heidelberg, Berlin, Heidelberg, 191–209. DOI: https://doi.org/10.1007/978-3-642-33573-0_12

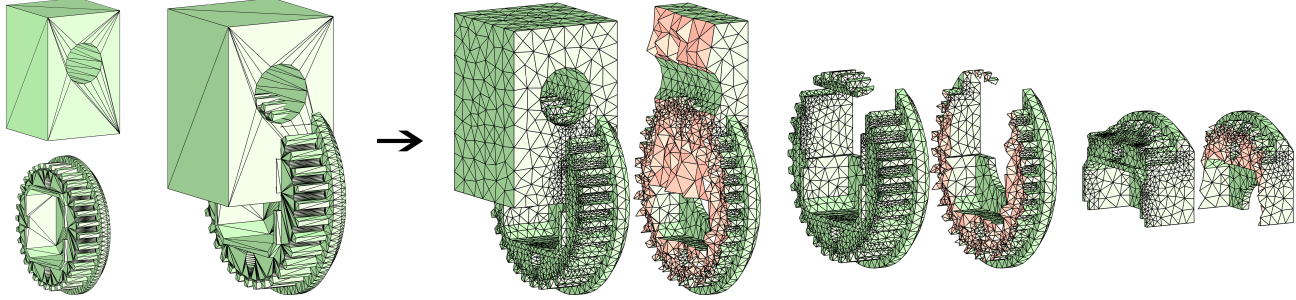


Fig. 13. Three Boolean operations computed on non-manifold, self-intersecting, and non-PWN input surface. The left is the input and the right are our output meshes after computing the union, difference, and intersection between the two models. The average timing is 39s and average max AMIPS energy is 8, with small variance between the operations.

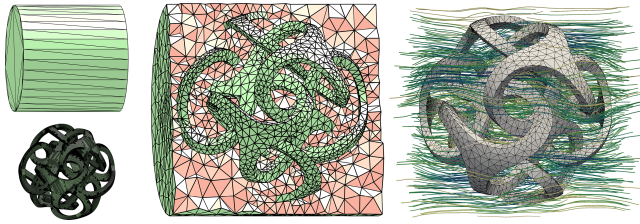


Fig. 14. Streamlines of a fluid (right) moving in a cylindrical pipe (top left) with a complicated obstacle (bottom left) in the center. The background mesh (middle, max AMIPS energy 9.5) is obtained by subtracting the obstacle from a cylinder using our method.

O. Busaryev, T. K. Dey, and J. A. Levine. 2009. Repairing and Meshing Imperfect Shapes with Delaunay Refinement. In *2009 SIAM/ACM Joint Conference on Geometric and Physical Modeling (SPM '09)*. ACM, New York, NY, USA, 25–33. DOI: <https://doi.org/10.1145/1629255.1629259>

M. Campen and L. Kobbelt. 2010. Exact and Robust (self-)intersections for Polygonal Meshes. *Comput. Graph. Forum* 29, 2 (2010), 397–406.

S. A. Canann, S. N. Muthukrishnan, and R. K. Phillips. 1996. Topological refinement procedures for triangular finite element meshes. *Engineering with Computers* 12, 3 (01 Sep 1996), 243–255. DOI: <https://doi.org/10.1007/BF01198738>

S. A. Canann, M. B. Stephenson, and T. Blacker. 1993. Optismoothing: An optimization-driven approach to mesh smoothing. *Finite Elements in Analysis and Design* 13, 2 (1993), 185 – 190. DOI: [https://doi.org/10.1016/0168-874X\(93\)90056-V](https://doi.org/10.1016/0168-874X(93)90056-V)

L. Chen and J.-c. Xu. 2004. Optimal Delaunay Triangulations. *Journal of Computational Mathematics* 22, 2 (2004), 299–308.

S.-W. Cheng, T. K. Dey, and J. A. Levine. 2008. A Practical Delaunay Meshing Algorithm for a Large Class of Domains. In *Proceedings of the 16th International Meshing Roundtable*. Springer, Berlin Heidelberg, Berlin, Heidelberg, 477–494.

S.-W. Cheng, T. K. Dey, and J. Shewchuk. 2012. *Delaunay Mesh Generation*. Chapman and Hall/CRC, Boca Raton, Florida.

L. P. Chew. 1989. Constrained delaunay triangulations. *Algorithmica* 4, 1 (01 Jun 1989), 97–108. DOI: <https://doi.org/10.1007/BF01553881>

L. P. Chew. 1993. Guarantee-Quality Mesh Generation for Curved Surfaces. In *Proceedings of the ninth annual symposium on Computational geometry - SCG '93*. ACM Press, New York, NY, USA, 274–280. DOI: <https://doi.org/10.1145/160985.161150>

D. Cohen-Steiner, E. C. de Verdière, and M. Yvinec. 2002. Conforming Delaunay Triangulations in 3D. In *Proceedings of the eighteenth annual symposium on Computational geometry - SCG '02*. ACM Press, New York, NY, USA, 217 – 233. DOI: <https://doi.org/10.1145/513400.513425>

J.-C. Cuilliere, V. Francois, and J.-M. Drouet. 2013. Automatic 3D Mesh Generation of Multiple Domains for Topology Optimization Methods. In *Proceedings of the 21st International Meshing Roundtable*. Springer Berlin Heidelberg, Berlin, Heidelberg, 243–259. DOI: https://doi.org/10.1007/978-3-642-33573-0_15

T. K. Dey and J. A. Levine. 2008. Delpsc: A Delaunay Mesh for Piecewise Smooth Complexes. In *Proceedings of the twenty-fourth annual symposium on Computational geometry - SCG '08*. ACM Press, New York, NY, USA, 220–221. DOI: <https://doi.org/10.1145/1377676.1377712>

A. Doi and A. Koide. 1991. An efficient method of triangulating equi-valued surfaces by using tetrahedral cells. *IEICE TRANSACTIONS on Information and Systems* 74, 1 (1991), 214–224.

C. Doran, A. Chang, and R. Bridson. 2013. Isosurface Stuffing Improved: Acute Lattices and Feature Matching. In *ACM SIGGRAPH 2013 Talks on - SIGGRAPH '13*. ACM Press, New York, NY, USA, 38:1–38:1. DOI: <https://doi.org/10.1145/2504459.2504507>

M. Douze, J.-S. Franco, and B. Raffin. 2015. *QuickCSG: Arbitrary and Faster Boolean Combinations of N Solids*. Technical Report 01121419, Inria Research Centre Grenoble, Rhône-Alpes.

Q. Du and D. Wang. 2003. Tetrahedral Mesh Generation and Optimization Based on Centroidal Voronoi Tessellations. *International journal for numerical methods in engineering* 56, 9 (2003), 1355–1373.

N. Faraj, J.-M. Thiery, and T. Boubekeur. 2016. Multi-Material Adaptive Volume Remesher. *Computer and Graphics Journal (proc. Shape Modeling International 2016)* 58 (2016), 150 – 160.

L. Feng, P. Alliez, L. Busé, H. Delingette, and M. Desbrun. 2018. Curved Optimal Delaunay Triangulation. *ACM Trans. Graph.* 37, 4 (2018), 61:1–61:16.

X.-M. Fu, Y. Liu, and B. Guo. 2015. Computing Locally Injective Mappings by Advanced MIPS. *ACM Trans. Graph.* 34, 4, Article 71 (July 2015), 12 pages. DOI: <https://doi.org/10.1145/2766938>

J. A. George. 1971. *Computer Implementation of the Finite Element Method*. Ph.D. Dissertation. Stanford University, Stanford, CA, USA. AAI205916.

M. Granados, P. Hachenberger, S. Hert, L. Kettner, K. Mehlhorn, and M. Seel. 2003. Boolean operations on 3D selective Nef complexes: Data structure, algorithms, and implementation. In *Proc. ESA*. Springer Berlin Heidelberg, Berlin, Heidelberg, 654–666.

G. Guennebaud, B. Jacob, and others. 2010. Eigen v3. (2010).

P. Hachenberger and L. Kettner. 2019. 3D Boolean Operations on Nef Polyhedra. In *CGAL User and Reference Manual* (4.14 ed.). CGAL Editorial Board. <https://doc.cgal.org/4.14/Manual/packages.html#PkgNef3>

R. Haines. 2014. MOSS: Multiple Orthogonal Strand System. In *Proceedings of the 22nd International Meshing Roundtable*. Springer International Publishing, Cham, 75–91. DOI: https://doi.org/10.1007/978-3-319-02335-9_5

K. Hu, D. Yan, D. Bommes, P. Alliez, and B. Benes. 2017. Error-Bounded and Feature Preserving Surface Remeshing with Minimal Angle Improvement. *IEEE Transactions on Visualization and Computer Graphics* 23, 12 (Dec 2017), 2560–2573. DOI: <https://doi.org/10.1109/TVCG.2016.2632720>

Y. Hu, T. Schneider, X. Gao, Q. Zhou, A. Jacobson, D. Zorin, and D. Panozzo. 2019. TriWild: Robust Triangulation with Curve Constraints. *ACM Trans. Graph.* (2019).

Y. Hu, Q. Zhou, X. Gao, A. Jacobson, D. Zorin, and D. Panozzo. 2018. Tetrahedral Meshing in the Wild. *ACM Trans. Graph.* 37, 4, Article 60 (July 2018), 14 pages. DOI: <https://doi.org/10.1145/3197517.3201353>

A. Jacobson, L. Kavan, and O. Sorkine-Hornung. 2013. Robust Inside-Outside Segmentation using Generalized Winding Numbers. *ACM Transactions on Graphics (proceedings of ACM SIGGRAPH)* 32, 4 (2013), 33:1–33:12.

C. Jamin, P. Alliez, M. Yvinec, and J.-D. Boissonnat. 2015. CGALmesh: A Generic Framework for Delaunay Mesh Generation. *ACM Trans. Math. Software* 41, 4 (10 2015), 1–24. DOI: <https://doi.org/10.1145/2699463>

F. Labelle and J. R. Shewchuk. 2007. Isosurface Stuffing: Fast Tetrahedral Meshes With Good Dihedral Angles. In *ACM SIGGRAPH 2007 papers on - SIGGRAPH '07*. ACM Press, New York, NY, USA, 57. DOI: <https://doi.org/10.1145/1275808.1276448>

B. Lévy. 2019. Geogram. (2019). <http://alice.loria.fr/index.php/software/4-library/75-geogram.html>

Y. Lipman. 2012. Bounded Distortion Mapping Spaces for Triangular Meshes. *ACM Trans. Graph.* 31, 4 (2012), 108.

W. E. Lorensen and H. E. Cline. 1987. Marching Cubes: A High Resolution 3D Surface Construction Algorithm. *SIGGRAPH Comput. Graph.* 21, 4 (Aug. 1987), 163–169. DOI: <https://doi.org/10.1145/37402.37422>

S. V. Magalhães, W. R. Franklin, and M. V. Andrade. 2017. Fast exact parallel 3D mesh intersection algorithm using only orientation predicates. In *Proceedings of the 25th ACM SIGSPATIAL International Conference on Advances in Geographic Information Systems*. ACM, ACM, New York, NY, USA, 44.

M. Mandad, D. Cohen-Steiner, and P. Alliez. 2015. Isotopic Approximation Within a Tolerance Volume. *ACM Trans. Graph.* 34, 4, Article 64 (July 2015), 12 pages. DOI: <https://doi.org/10.1145/2766950>

N. Molino, R. Bridson, and R. Fedkiw. 2003. Tetrahedral Mesh Generation for Deformable Bodies. In *Proc. Symposium on Computer Animation*.

M. Murphy, D. M. Mount, and C. W. Gable. 2001. A Point-Placement Strategy for Conforming Delaunay Tetrahedralization. *International Journal of Computational Geometry & Applications* 11, 06 (12 2001), 669–682. DOI: <https://doi.org/10.1142/s0218195901000699>

K. Museth, D. E. Breen, R. T. Whitaker, and A. H. Barr. 2002. Level set surface editing operators. *ACM Trans. Graph.* 21, 3 (2002), 330–338.

B. Naylor, J. Amanatides, and W. Thibault. 1990. Merging BSP trees yields polyhedral set operations. In *Proc. SIGGRAPH*. ACM, New York, NY, USA, 115–124.

A. Paoluzzi, V. Shapiro, and A. DiCarlo. 2017. Arrangements of cellular complexes. *CoRR* abs/1704.00142 (2017). arXiv:1704.00142 <http://arxiv.org/abs/1704.00142>

D. Pavic, M. Campen, and L. Kobbelt. 2010. Hybrid Booleans. *Comput. Graph. Forum* 29 (2010), 75–87.

J. Peraire, M. Vahdati, K. Morgan, and O. C. Zienkiewicz. 1987. Adaptive Remeshing for Compressible Flow Computations. *J. Comput. Phys.* 72, 2 (Oct. 1987), 449–466. DOI: [https://doi.org/10.1016/0021-9991\(87\)90093-3](https://doi.org/10.1016/0021-9991(87)90093-3)

M. Rabinovich, R. Poranne, D. Panozzo, and O. Sorkine-Hornung. 2017. Scalable Locally Injective Mappings. *ACM Trans. Graph.* 36, 2 (April 2017), 16. DOI: <https://doi.org/10.1145/2983621>

J.-F. Remacle. 2017. A Two-Level Multithreaded Delaunay Kernel. *Computer-Aided Design* 85 (04 2017), 2–9. DOI: <https://doi.org/10.1016/j.cad.2016.07.018>

J. Ruppert. 1995. A Delaunay Refinement Algorithm for Quality 2-Dimensional Mesh Generation. *Journal of Algorithms* 18, 3 (05 1995), 548–585. DOI: <https://doi.org/10.1006/jagm.1995.1021>

E. A. Sadek. 1980. A scheme for the automatic generation of triangular finite elements. *Internat. J. Numer. Methods Engrg.* 15, 12 (1980), 1813–1822. DOI: <https://doi.org/10.1002/nme.1620151206> arXiv: <https://onlinelibrary.wiley.com/doi/pdf/10.1002/nme.1620151206>

R. Schmidt and K. Singh. 2010. Meshmixer: an interface for rapid mesh composition. In *ACM SIGGRAPH 2010 Talks*. ACM, ACM, New York, NY, USA, 6.

T. Schneider, Y. Hu, J. Dumas, X. Gao, D. Panozzo, and D. Zorin. 2018. Decoupling simulation accuracy from mesh quality. *ACM Transactions on Graphics* 37, 6 (dec 2018), 1–14. DOI: <https://doi.org/10.1145/3272127.3275067>

M. Schweiger and S. Arridge. 2016. Basis mapping methods for forward and inverse problems: BASIS MAPPING METHODS. *Internat. J. Numer. Methods Engrg.* 109 (05 2016). DOI: <https://doi.org/10.1002/nme.5271>

D. R. Sheehy. 2012. New Bounds on the Size of Optimal Meshes. *Computer Graphics Forum* 31, 5 (08 2012), 1627–1635. DOI: <https://doi.org/10.1111/j.1467-8659.2012.03168.x>

B. Sheng, P. Li, H. Fu, L. Ma, and E. Wu. 2018a. Efficient non-incremental constructive solid geometry evaluation for triangular meshes. *Graphical Models* 97 (2018), 1–16.

B. Sheng, B. Liu, P. Li, H. Fu, L. Ma, and E. Wu. 2018b. Accelerated robust Boolean operations based on hybrid representations. *Computer Aided Geometric Design* 62 (2018), 133–153.

J. Shewchuk. 2012. *Unstructured Mesh Generation*. Chapman and Hall/CRC, Boca Raton, Florida, Chapter 10, 257 – 297.

J. R. Shewchuk. 1996. Triangle: Engineering a 2D quality mesh generator and Delaunay triangulator. In *Applied Computational Geometry Towards Geometric Engineering*, Ming C. Lin and Dinesh Manocha (Eds.). Springer Berlin Heidelberg, Berlin, Heidelberg, 203–222.

J. R. Shewchuk. 1997. Adaptive Precision Floating-Point Arithmetic and Fast Robust Geometric Predicates. *Discrete & Computational Geometry* 18, 3 (Oct. 1997), 305–363.

J. R. Shewchuk. 1998. Tetrahedral Mesh Generation by Delaunay Refinement. In *Proceedings of the fourteenth annual symposium on Computational geometry - SCG '98*. ACM Press, New York, NY, USA, 86–95. DOI: <https://doi.org/10.1145/276884.276894>

J. R. Shewchuk. 1999. Lecture Notes on Delaunay Mesh Generation. (1999).

J. R. Shewchuk. 2002. Constrained Delaunay Tetrahedralizations and Provably Good Boundary Recovery. In *Eleventh International Meshing Roundtable*. Sandia National Laboratories, 193–204.

H. Si. 2015. TetGen, a Delaunay-Based Quality Tetrahedral Mesh Generator. *ACM Trans. Math. Softw.* 41, 2, Article 11 (Feb. 2015), 36 pages. DOI: <https://doi.org/10.1145/2629697>

H. Si and K. Gartner. 2005. Meshing Piecewise Linear Complexes by Constrained Delaunay Tetrahedralizations. In *Proceedings of the 14th international meshing roundtable*. Springer, Springer Berlin Heidelberg, Berlin, Heidelberg, 147–163.

H. Si and J. R. Shewchuk. 2014. Incrementally Constructing and Updating Constrained Delaunay Tetrahedralizations With Finite-Precision Coordinates. *Engineering with Computers* 30, 2 (04 2014), 253–269. DOI: <https://doi.org/10.1007/s00366-013-0331-0>

W. C. Thibault and B. F. Naylor. 1987. Set operations on polyhedra using binary space partitioning trees. In *Proc. SIGGRAPH*. ACM, New York, NY, USA, 153–162.

J. Tournais, C. Wormser, P. Alliez, and M. Desbrun. 2009. Interleaving Delaunay Refinement and Optimization for Practical Isotropic Tetrahedron Mesh Generation. *ACM Transactions on Graphics* 28, 3 (07 2009), 1. DOI: <https://doi.org/10.1145/1531326.1531381>

G. Varadhan, S. Krishnan, T. Sriram, and D. Manocha. 2004. Topology preserving surface extraction using adaptive subdivision. In *SGP*. ACM, New York, NY, USA, 235–244.

C. C. L. Wang. 2011. Approximate Boolean Operations on Large Polyhedral Solids with Partial Mesh Reconstruction. *IEEE Trans. Vis. Comput. Graph.* 17, 6 (2011), 836–849.

R. Wein, E. Berberich, E. Fogel, D. Halperin, M. Hemmer, O. Salzman, and B. Zukerman. 2018. 2D Arrangements. In *CGAL User and Reference Manual* (4.13 ed.). CGAL Editorial Board. <https://doc.cgal.org/4.13/Manual/packages.html#PkgArrangement2Summary>

M. A. Yerry and M. S. Shephard. 1983. A Modified Quadtree Approach To Finite Element Mesh Generation. *IEEE Computer Graphics and Applications* 3, 1 (Jan 1983), 39–46. DOI: <https://doi.org/10.1109/MCG.1983.262997>

H. Zhao, C. C. Wang, Y. Chen, and X. Jin. 2011. Parallel and efficient Boolean on polygonal solids. *The Visual Computer* 27, 6–8 (2011), 507–517.

Q. Zhou, E. Grinspun, D. Zorin, and A. Jacobson. 2016. Mesh Arrangements for Solid Geometry. *ACM Transactions on Graphics (TOG)* 35, 4 (2016), 39.

Q. Zhou and A. Jacobson. 2016. Thingi10K: A Dataset of 10, 000 3D-Printing Models. *CoRR* abs/1605.04797 (2016). arXiv:1605.04797